Seismic risk assessment of as-built and retrofitted non-ductile reinforced concrete frames

P. Vega-Behar, C.S.W. Yang, & R. DesRoches
Georgia Institute of Technology, Atlanta, Georgia, USA

R.T. Leon
Virginia Polytechnic Institute and State University, Blacksburg, Virginia, USA

ABSTRACT: Reinforced concrete (RC) frames, exhibiting non-ductile behavior, have been widely used in low-to-moderate seismic zones in the US. Several retrofits schemes and techniques have been developed to address deficiencies in these structures. However, the efficiency of these retrofits depends on several factors. As part of a large scale project that aims to validate classes of retrofits for these buildings, this paper presents the risk assessment of three sample buildings. The buildings represent (1) an as-built, pre-1970s RC frame, (2) said frame with retrofitted columns to address deficient lap splices, and (3) the frame with a retrofitted beam-column joint region to prevent slip of inadequately anchored beam reinforcement. Fragility curves are developed using nonlinear time history analysis and are used to evaluate and compare the vulnerability of the frames. Results show that retrofitting the columns improves the seismic performance, while retrofitting the joints without addressing column deficiencies decreases performance.

1 INTRODUCTION

Reinforced concrete (RC) gravity frames (Fig. 1), exhibiting non-ductile behavior, have been widely used for building construction in low-to-moderate seismic zones in the US (Celik & Ellingwood 2009, Jeon et al. 2012, Ramamoorthy et al. 2006). Over past decades, retrofit schemes and techniques have been used to address ductility, strength, and stiffness deficiencies in these structures. Some conventional schemes (FEMA 2006) used in the practice include addition of new elements (e.g. braces, shear walls) and strengthening/stiffening of existing elements (e.g. column wrapping). While proven effective, the degree of efficiency of these retrofits varies depending on factors like seismic risk, building accessibility and occupancy.

The present study is part of a project that aims to validate retrofit techniques for RC buildings via large scale testing. The objectives of the analysis presented in this paper are (1) to aid in the selection of retrofits for experimental testing by identifying vulnerable components and possible retrofit techniques, and (2) to provide a basis for refined vulnerability models updated with results from aforementioned experimental tests.

This paper presents the seismic risk assessment of as-built and retrofitted non-ductile RC frames. The analytical modeling of an as-built frame and two frames considering retrofitted vulnerable components is shown. Nonlinear time history analysis is performed to develop fragility curves for all buildings. The results from the analytical fragility curves are used to compare the seismic performance of the three frames.

Figure 1. Typical central US pre-1970's RC frame building.

2 ANALYTICAL MODELING OF VULNERABLE RC FRAME COMPONENTS

The full-scale experimental test setup that will be built as part of this project (hereby referred to as 'test frame') consists of four identical 2-story, 2-bay RC frames designed to resemble typical RC frame construction in the central and southeastern US

(CSUS) prior to the 1970's. The ACI 318-63 Building Code (ACI 1963) and the CRSI Design Handbook, Volume II, 1963 ACI Code (Reese 1965) were used throughout the design process. In this study, all modeling parameters are selected to match the test frame design. Frame elevation is shown in Figure 2. Geometry and reinforcement layouts of beams and columns are shown in Figure 3.

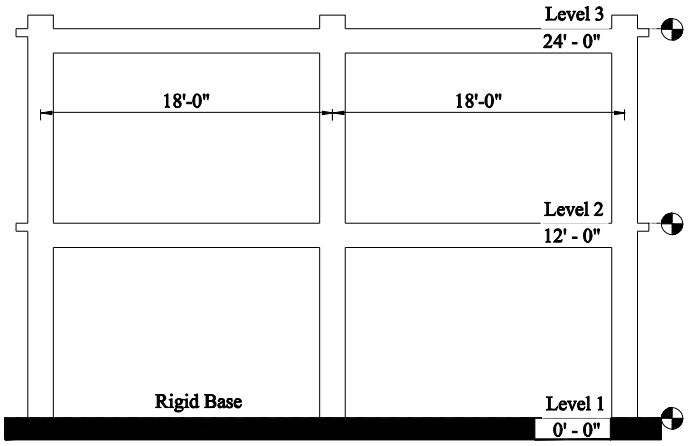

Figure 2. Test frame – elevation view.

In accordance to typical practice at the time (Bracci et al. 1992), no consideration was given to lateral loads during the design. While structures designed for gravity loads still possess inherent lateral strength that may be capable of resisting moderate earthquakes (Hoffmann et al. 1992, Kunnath et al. 1995), potential deficiencies in detailing of members may result in poor performance during seismic activity (ACI 2002, Beres et al. 1992, Bracci et al. 1995). For example, Beres et al. (1992) identified the following details as potentially critical to safety during an earthquake: (1) longitudinal reinforcement ratio in columns not exceeding 2%, (2) lap splices of column reinforcement at the maximum moment region, (3) wide spacing of column ties that provides little concrete confinement, (4) little to no transverse reinforcement within the joint region, (5) bottom beam reinforcement with a short embedment length into the column, (6) construction joints near the beam-column joints, and (7) columns having bending moment capacities close to those of the beams. All deficiencies except (1) and (6) were considered in this study.

For this study, nonlinear finite element analysis was performed in OpenSees (McKenna et al. 2010). Finite element modeling allows for explicit consideration of column and beam moment capacities. To capture the effects of other deficiencies, component and material models validated by previous researchers were incorporated into the structural frame. A general overview of these models is shown next. For detailed descriptions, the reader is referred to the corresponding studies.

Lap splices in regions of maximum moment (e.g. just above the foundation – Fig. 3) have been shown to contribute to strength and stiffness degradation in columns (Aboutaha et al. 1996, Melek & Wallace 2004). Barkhoradary & Tariverdilo (2011) developed an analytical model to capture this degrading behavior. The model was validated with experimental tests from Melek & Wallace (2004) and Aboutaha et al. (1996). These tests had column geometry and reinforcement layouts comparable to those of the test frame columns (e.g. 24" lap splice length, #8 rebars). Therefore, the model of Barkhoradary & Tariverdilo is used in this study. The spliced reinforcement backbone relationship is shown in Figure 4. Corresponding parameters are shown in Table 1.

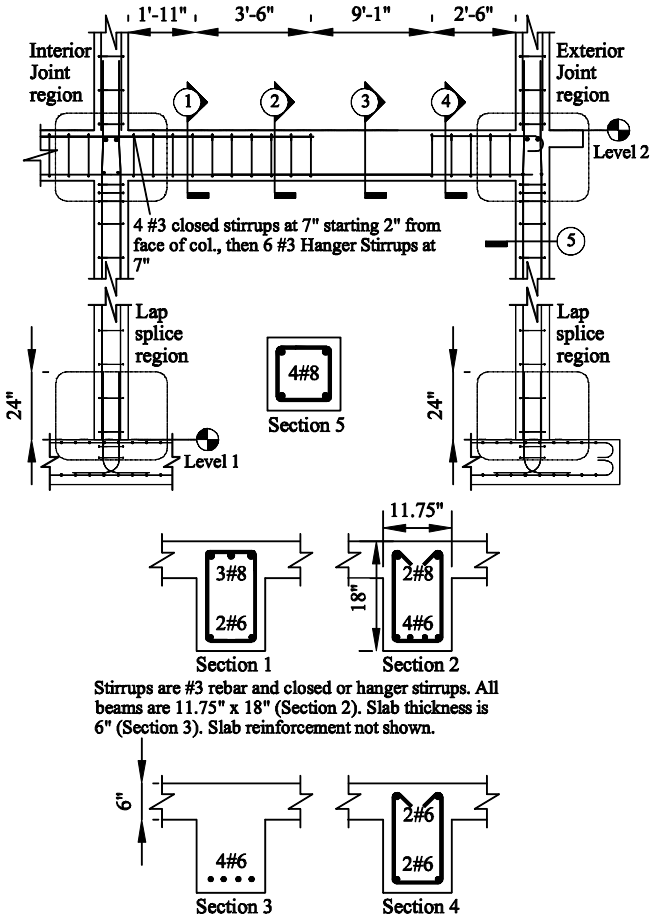

Figure 3. Beam and column geometry and reinforcement details (not to scale).

To assess the performance of the beam-column joint region, joint shear behavior and poor anchorage of beam reinforcement are considered. The model proposed by Celik & Ellingwood (2008) is used to establish a joint moment-rotation (M-θ) relationship. The M-θ backbone is derived from the shear stress-strain relationship of the joint using the joint geometry and equilibrium as described in Equation 1:

$$M_j = \frac{\nu_j A_j}{(1-b_j/L_b)/jd_b - \alpha/L_c},\ \theta_j = \gamma_j \qquad (1)$$

where M_j = equivalent joint rotational moment; v_j = joint shear stress; b_j = joint effective width; A_j = joint area; L_b = beam total length; L_c = column total length; j = internal moment arm factor (assumed to be 0.875); d_b = beam effective depth; α = constant equal to 2 for the top floor joints and 1 for the others; θ_j = joint rotation; and γ_j = joint shear strain. Since the joint rotation is the angle change between the two adjacent edges of the panel zone, the joint rotation equals the joint shear strain. Figure 4 depicts the joint rotational spring M-θ retlationship. Joint rotation (θ) values are shown in Table 2.

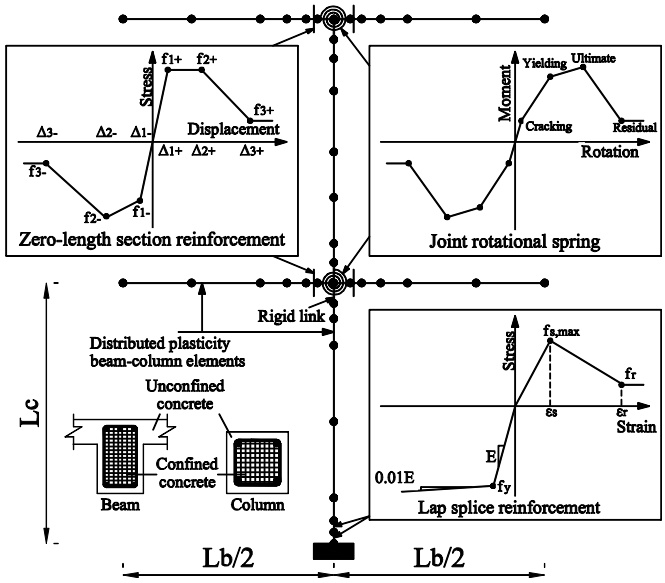

Figure 4. Element discretization around interior column. Material constitutive curves (not to scale) shown for joint rotational spring, lap-splice reinforcement, and zero-length section bottom reinforcement.

Table 1. Lap splice reinforcement parameters

$f_{s,max}/f_y$	ε_s	f_r/f_y	ε_r
0.71	0.0047	0.39	0.035

Celik & Ellingwood calibrated their model against a series of experimental sub-assembly tests with no transverse reinforcement in the joint. The tests included joints with well anchored beam reinforcement (Walker 2001) as well as beam reinforcement with short embedment lengths (Pantelides et al. 2002). For beams with poorly anchored bottom reinforcement, the joint M-θ envelope was reduced to account for the decreased beam negative moment capacity. However, additional rotation due to reinforcement slip was ignored.

Table 2. Joint rotational spring parameter, θ (rad)*

Cracking	Yielding	Ultimate	Residual
0.0007	0.006	0.02	0.065

*θ values chosen from empirical data (Celik & Ellingwood 2008)

Unlike the Celik & Ellingwood model, no strength reduction factor is assigned to the joint rotational spring in the present study. Instead, the behavior of beam reinforcement with short embedment length is considered using a bond slip displacement model formulated by Berry & Eberhard (2008). In this model, the OpenSees *zeroLengthSection* element is assigned to beam ends at the joint face. The *zeroLengthSection* allows for explicit modeling of the section geometry and reinforcement, but the materials are given a stress-displacement (σ-Δ), rather than stress-strain, relationship. The concrete σ-Δ envelope follows the formulation of Berry & Eberhard, while the bottom steel reinforcement σ-Δ (values shown in Table 3) was formulated using bond values proposed by Mitra & Lowes (2007). Figure 4 shows the stress-displacement curve for the beam bottom steel reinforcement.

It is assumed that accounting for joint shear behavior and reinforcement slip separately (as described above) allows for more flexibility when modeling the test frame in a retrofitted state. To ensure that appropriate behavior of the joint region was captured, analytical and experimental results of interior and exterior joint subassemblies were compared. The joint model described above (rotational spring plus *zeroLengthSection* σ-Δ element) was compared to results from Celik & Ellingwood (2008), and the corresponding experimental tests (Walker 2001, Pantelides et al. 2001). Analytical results from this study's joint model are well correlated with aforementioned analytical and experimental results.

The model of Mander et al. (1988) was used to account for differences in ductility and compressive strength of confined and unconfined concrete. Only the sections with closed stirrups (cross-sections 1 and 5 in Fig. 3) were assumed to have confined cores. Joint moment-rotation relationships were calculated using moment-curvature analysis for every connection and the effective slab width was defined according to the recommendations of ACI 318-05 Building Code (ACI 2005).

Table 3. Zero-length section reinforcement (beam bottom rebar) parameters

Stress					
f_{1+}/f_y	f_{2+}/f_y	f_{3+}/f_y	f_{1-}/f_y	f_{2-}/f_y	f_{3-}/f_y
0.64	0.64	0.15	-0.78	-1.25	-0.15
Displacement					
Δ_{1+} (in)	Δ_{2+} (in)	Δ_{3+} (in)	Δ_{1-} (in)	Δ_{2-} (in)	Δ_{3-} (in)
0.0049	0.1181	0.4143	-0.0049	-0.1181	-0.4143

3 AS-BUILT TEST FRAME FRAGILITY

This section covers the seismic vulnerability assessment of the as-built test frame. It includes descriptions of the ground motion suite and probabilistic parameters used in the seismic demand analysis, and the development of fragility curves.

3.1 *Probabilistic analytical models*

The full analytical model of the test frame was built in OpenSees. In addition to component models described in the previous section, distributed plasticity elements were used to model columns and beams. For dynamic analysis, mass was lumped at every beam-column connection. Mass and stiffness proportional Rayleigh damping was considered in the first two modes. The critical damping ratio was assumed to follow a lognormal distribution with a mean value of 0.04 (Newmark & Hall, 1982) and a 25% coefficient of variation for a corresponding normal distribution (Healey et al. 1980). Mean concrete compressive strength and steel yield strength were increased by 25% from their nominal values to account for conservatism in nominal to in-situ strength and apparent strength increase under seismic loading rates (Aslani & Miranda, 2005).

The test frame was designed (and will be tested experimentally) assuming two-way slab action. A concrete unit weight of 145 pcf was assumed for self-weight calculations. A triangularly distributed load was assigned to the beams during the design process. OpenSees only allows modeling of uniformly distributed loads. Thus, triangular gravity loads were discretized into uniform loads for each individual beam element as shown in Figure 5.

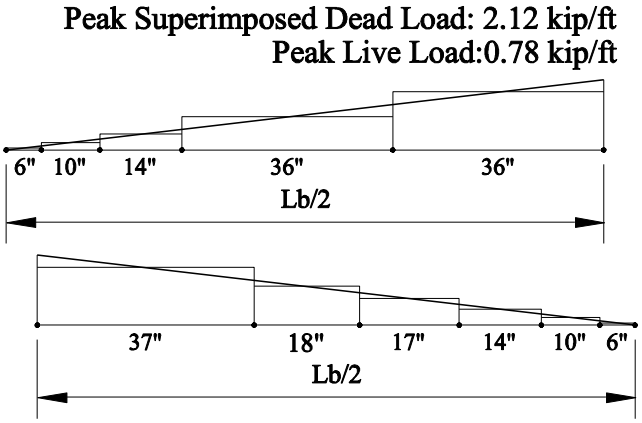

Figure 5. Gravity load discretization. Note that this arrangement corresponds to the beams on the left bay of the test frame. The frame is symmetric about the interior column.

Uncertainty in modeling parameters was considered using a Latin Hypercube sampling technique (McKay et al. 1979). The concrete compressive strength (f_c), steel yield strength (f_y), and damping ratio (ζ) were treated as random variables with the associated probability distributions shown in Table 4. Considering the uncertainties, eigenvalue analysis revealed a range of fundamental periods from 0.42 s to 0.64 s for the 240 frames.

Table 4. Modeling uncertainties

RVs	Mean	COV	Distribution	
f_c (ksi)	5.0	0.18	Normal	Healy et al. (1980)
f_y (ksi)	75.0	0.11	Lognormal	
ζ	0.05	0.25	Lognormal	*

*Damping ratio parameters were chosen for agreement with those suggested by Healey et al. (1980), Newmark & Hall (1982), and Nielson & DesRoches (2007).

3.2 *Ground motion suite*

A suite of 240 synthetic ground motions developed by Fernandez & Rix (2006) are used to perform NTHA. These probabilistic ground motions were generated for eight cities within the upper Mississippi Embayment. The suite contains ground motions consistent with hazard levels of 10%, 5%, and 2% probability of exceedance in 50 years and is considered representative of the seismic hazard in the CSUS.

3.3 *Probabilistic seismic demand model (PSDM)*

The 240 Rix-Fernandez ground motions are randomly paired with 240 test frame models to create 240 frame – ground motion pairs which are statistically significant and nominally identical. A full NTHA is performed for each frame – ground motion pair and the maximum structural demand (e.g. interstory drift) is recorded. A seismic intensity measure (IM) is chosen. Then, assuming that the median seismic demand can be predicted from a power law model (Cornell et al. 2002), a linear regression of the demand-intensity measure pairs is performed in the log-transformed space. The regression is used to formulate the so called PSDM in terms of a lognormal distribution. Several researchers have studied the effects of using different IMs. A summary may be found in Padgett et al. (2008).

In this study, the peak ground acceleration (PGA) and spectral acceleration at the fundamental period of the frame ($S_{a\text{-}T1}$), at 1 s ($S_{a\text{-}1.0s}$), and at 0.2 s ($S_{a\text{-}0.2s}$) are chosen as IMs for the as-built frame. Figure 6 shows the PSDMs for maximum interstory drift (θ_{max}) as a function of the aforementioned IMs. Comparing the IMs shows that $S_{a\text{-}1}$ is the most efficient (lowest dispersion, $\beta_{d|IM}$). Thus, this demand model will be used to develop fragility curves for the as-built frame, as well as the frame with components in a retrofitted state. For a detailed description on the choice of optimal IM, refer to Padgett et al. (2008).

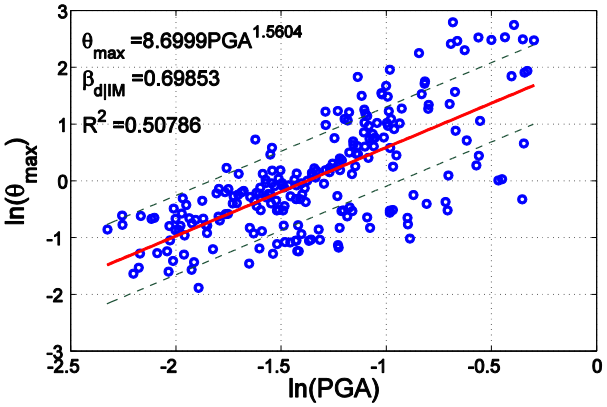

(a) PSDM with peak ground acceleration IM

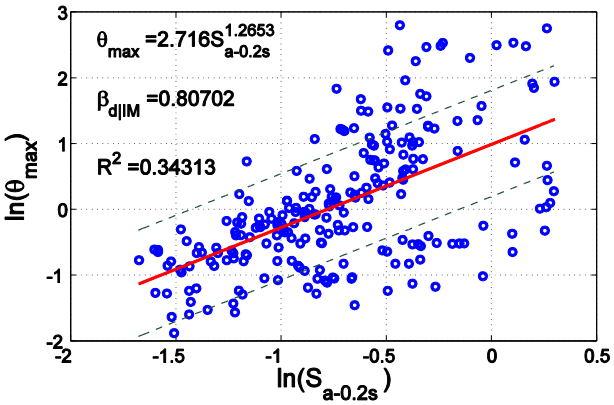

(b) PSDM with spectral acceleration (at 0.2 s) IM

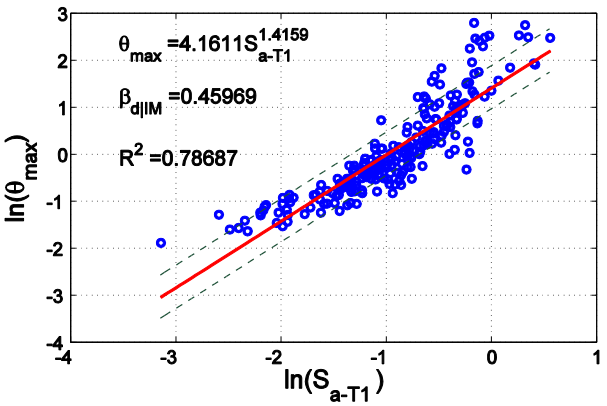

(c) PSDM with spectral acceleration (at T1) IM

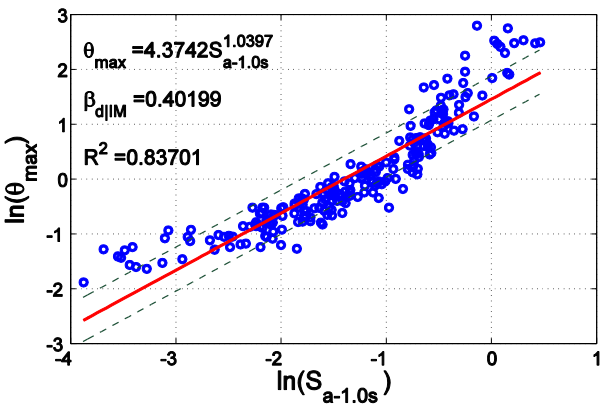

(d) PSDM with spectral acceleration (at 1 s) IM

Figure 6. PSDMs for as-built test frame.

A total of 10 NTHA failed to reach a convergent solution for the as-built frame. There were 7 such cases for the test frame with retrofitted joints and none for the frame with retrofitted columns. Following the recommendations of Taftali (2007), these cases are considered structural "collapses" and are excluded from the data set on which the regression analysis is performed.

3.4 *Capacity limit states*

The capacity limit state for maximum interstory drift (%) is also assumed to be lognormally distributed. The median values obtained from HAZUS-MH (FEMA, 2003) are 0.5, 0.8, 2.0, and 5.0 for the slight, moderate, extensive, and complete damage states, respectively. The prescriptive capacity dispersions for the lower and higher limit states are 0.25, and 0.47, respectively.

3.5 *Fragility Curves*

Fragility curves consider the probability that the seismic demand (D) placed on the structure exceeds the capacity (C) conditioned on the chosen IM. Having defined the PSDMs and limit states as described in the previous sections, the fragility is evaluated as in Equation 2:

$$P[D > C \mid IM] = \Phi\left[\frac{\ln(S_d / S_c)}{\sqrt{\beta_{d|IM}^2 + \beta_c^2 + \beta_m^2}}\right] \qquad (2)$$

where S_d and $\beta_{d|IM}$ = median value and dispersion of the demand as a function of *IM*, respectively; S_c and β_c = median value and dispersion of the capacity limit states, respectively; β_m is the modeling uncertainty (assumed to be 0.2, Celik & Ellingwood 2010) and $\Phi[\cdot]$ = standard normal cumulative distribution function. Figure 7 illustrates the fragility curves for the as-built test frame using $S_{a\text{-}1.0s}$ as the IM.

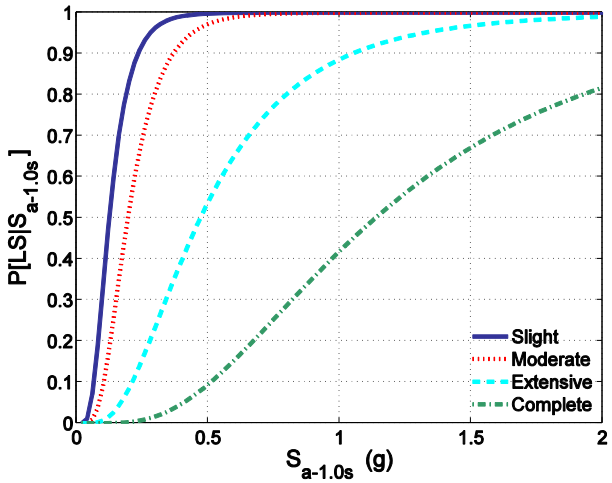

Figure 7. Fragility curves for as-built test frame

4 FRAGILITY ESTIMATES OF RETROFITTED TEST FRAME

To aid in selection of experimental retrofits, several cases of a retrofitted building must be analyzed and compared to the as-built test frame. Two fragility estimates of the test frame in a retrofitted state are presented in the following sections. Section 4.1 presents the PSDM and fragility curves for the test frame considering a retrofitted column lap splice region (Fig. 3). Fragility of frame with a retrofitted beam-column joint region (Fig. 3) is shown in section 4.2.

4.1 *Fragility of frame with retrofitted lap splice*

Previous research has shown that retrofitting columns with deficient lap splices via column jacketing along the splice length may effectively prevent lap splice failures (ElGawady et al. 2010). Thus, a retrofitted column was modeled by assigning a reinforcing steel material with strain hardening (i.e. *Steel02* in OpenSees) to the lap splice region, rather than the constitutive relation shown in Figure 4. Figure 8 and Figure 9 show the PSDM and fragility curves, respectively, for the test frame with retrofitted lap splice regions.

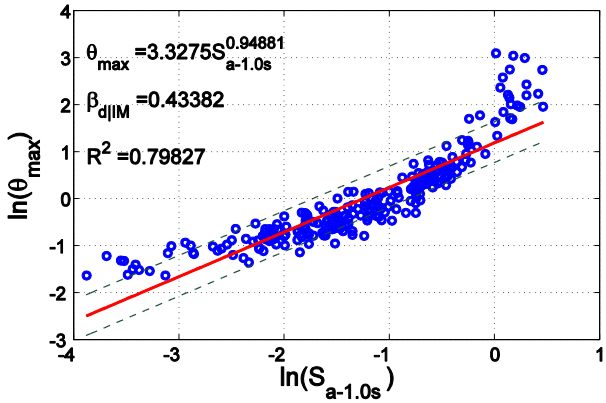

Figure 8. PSDM for test frame with retrofitted lap splice

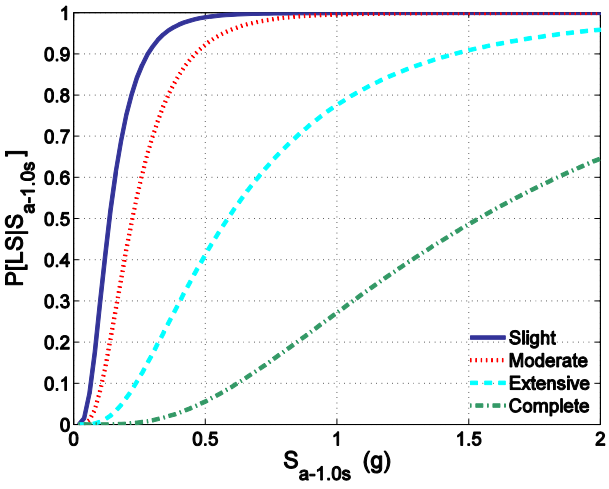

Figure 9. Fragility curves for test frame with retrofitted lap splice region

4.2 *Fragility of frame with retrofitted beam column joints*

For the purpose of an initial fragility estimate, it is assumed that a retrofitted beam-column joint region may prevent additional beam rotation due to reinforcement slip. Such a retrofit may also allow the beams to develop a larger fraction of their flexural capacity (FEMA 2006, Bracci et al. 1995). For modeling purposes, this behavior is achieved by removing the *zeroLengthSection* element (Fig. 4) from the analytical model. The PSDM conditioned on $S_{a\text{-}1.0s}$ is shown in Figure 10. Fragility curves were calculated for the same four limits states described in Section 3.4. The fragility curves are shown in Figure 11.

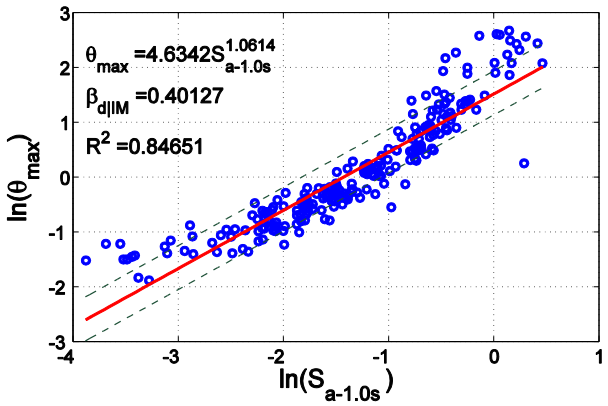

Figure 10. PSDM for test frame with retrofitted joints

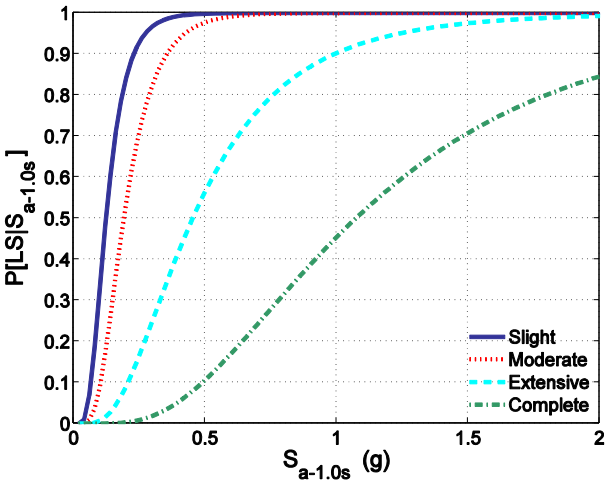

Figure 11. Fragility curves for test frame with retrofitted joints

4.3 *Comparison of fragility curves for as-built and retrofitted test frames*

Table 5 shows the median spectral acceleration values for all limit states in the three structures presented in this paper. It can be seen that retrofitting the joint region without retrofitting the column worsens the seismic performance. The median ground motion that will exceed the complete damage state decreases from 1.137g for the as-built frame to 1.074g to the frame with retrofitted joints (a 5.5% decrease).

Conversely, a retrofit in the lap splice region significantly improves the seismic performance across all limit states.

Table 5. Median spectral acceleration values

Structure	Slight (g)	Moderate (g)	Extensive (g)	Complete (g)
As-built	0.124	0.195	0.471	1.137
Retrofitted joints	0.123	0.191	0.453	1.074
Retrofitted splice	0.136	0.223	0.585	1.536

5 SUMMARY AND CONCLUDING REMARKS

The seismic fragility assessment of a 2-story, 2-bay non-ductile RC building was carried out using NTHA. This structure is representative of pre-1970's construction in low-to-moderate seismic zones in the US. Thus, several reinforcement detailing deficiencies were considered in the as-built frame analytical model. To aid in the selection of retrofits for future experimental testing and establish a basis for further modeling of retrofits, two of these deficiencies, namely short lap splices near the column foundation and inadequate anchorage of beam reinforcement, were also modeled in a retrofitted state. Preliminary fragility estimates were developed for the structure in three conditions: as-built, with retrofitted column lap splices, and with retrofitted beam-column joints.

Under the assumed interstory drift-IM relationship, the 5% spectral acceleration at 1 s provided the most efficient PSDM. This is indicative of global stiffness degradation since there is more dispersion in the PSDM conditioned on spectral acceleration at the fundamental period of the undamaged structure. That said, there is a large amount of dispersion in the upper range of ground motion intensity for both IMs. Several data points in this region lie outside the one-standard deviation value of the regression model and above a 10% interstory drift level. Further research and updating with experimental data is required to improve the accuracy of these values.

Retrofitting the column lap splice region improved the seismic performance for all limit states. This result indicates that the as-built structure is strongly affected by an inadequate beam-to-column strength ratio (i.e. a 'strong-beam weak-column' design).

The probability of exceeding the complete damage state increased slightly for a structure with retrofitted beam-column joints. Further research is needed to determine if this result is a product of the chosen PSDM, or if the increase in the beam-to-column strength ratio (due to the beam developing a larger proportion of its ultimate strength) caused a corresponding increase in the drift demand.

6 ACKNOWLEDGEMENTS

This research was supported by the National Science Foundation under Grant CMMI-1041607. However, the views expressed are solely those of the authors and may not represent the position of the NSF.

7 REFERENCES

Aboutaha, R.S., Engelhardt, M.D., Jirsa, J.O. & Kerger, M.E. 1996. Retrofit of concrete columns with inadequate lap splices by the use of rectangular steel jackets. *Earthquake Spectra* 12(4): 693-714.

ACI Committee 318. 1963. *Building Code Requirements for Reinforced Concrete (ACI 318-63)*. Detroit, MI: American Concrete Institute.

ACI Committee 318. 2005. *Building Code Requirements for Structural Concrete (ACI 318-05) and Commentary (ACI 318R-05)*. Detroit, MI: American Concrete Institute.

ACI Committee 352. 2002. *Recommendations for Design of Beam-Column Connections in Monolithic Reinforced Concrete Structures (ACI 352R-02)*. Detroit, MI: American Concrete Institute.

Aslani, H. & Miranda, E. 2005. Probability-based seismic response analysis. *Engineering Structures* 27(8): 1151-1163.

Barkhoradary, M. & Tariverdilo, S. 2011. Vulnerability of ordinary moment resistant concrete frames. *Earthquake Engineering & Engineering Vibrations* 10(4): 519-533.

Beres, A., White, R.N. & Gergely, P 1992. Seismic behavior of reinforced concrete frame structures with nonductile details: Part I – Summary of experimental findings of full scale beam-column joint tests. *Technical Report NCEER-92-0024* National Center for Earthquake Engineering Research, State University of New York at Buffalo, Buffalo, NY.

Berry, M.P. & Eberhard, M.O. 2008. Performance modeling strategies for modern reinforced concrete bridge columns. *PEER Report 2007/07* Pacific Earthquake Engineering Center, University of California, Berkeley, CA.

Bracci, J.M., Reinhorn A.M. & Mander, J.B. 1992. Seismic resistance of reinforced concrete frame structures designed only for gravity loads – Part I: Design and properties of a 1/3 scale model structure. *Technical Report NCEER-92-0027* National Center for Earthquake Engineering Research, State University of New York at Buffalo, Buffalo, NY.

Bracci, J.M., Reinhorn A.M. & Mander, J.B. 1995. Seismic retrofit of reinforced concrete buildings designed for gravity loads: performance of the structural model. *ACI Structural Journal* 92(6): 711-722.

Celik, O.C. & Ellingwood, B.R. 2008. Modeling beam-column joints in fragility assessment of gravity load designed reinforced concrete frames. *Journal of Earthquake Engineering* 12(3): 357-381.

Celik, O.C. & Ellingwood, B.R. 2009. Seismic risk assessment of gravity load designed reinforced concrete frames subjected to mid-America ground motions. *ASCE Journal of Structural Engineering* 135(4): 414-424.

Celik, O.C. & Ellingwood, B.R. 2010. Seismic fragilities for non-ductile reinforced concrete frames – Role of aleatoric and epistemic uncertainties. *Structural Safety* 32: 1-12.

Cornell, C.A., Jalayer, F., Hamburger, R.O., & Foutch, D.A. 2002. Probabilistic basis for 2000 SAC Federal Emergency Management Agency steel moment frame guidelines. *ASCE Journal of Structural Engineering* 128(4): 526-533.

ElGawady M., Mesay, E., McLean, D. & Sack, R. 2010. Retrofitting of rectangular columns with deficient lap splices. *ASCE Journal of composites for construction* 14(1): 22-35.

Federal Emergency Management Agency 2003. Multi-hazard loss estimation methodology, Earthquake model. *HAZUS-MH MR1 Technical Manual*, Washington, DC: FEMA.

Federal Emergency Management Agency 2006. *Techniques for the seismic rehabilitation of existing buildings (FEMA 547)*. Washington, DC: FEMA.

Healy, J.J., Wu, S.T. & Murga M. 1980. *Structural building response review*. NUREG/CR-1423, Vol. 1, US Nuclear Regulatory Commission, Washington, DC.

Hoffman, G.W., Kunnath, S.K., Reinhorn, A.M. & Mander, J.B. 1992. Gravity-load-designed reinforced concrete buildings: Seismic evaluation of existing construction and detailing strategies for improved seismic resistance. *Technical Report NCEER-92-0016* National Center for Earthquake Engineering Research, State University of New York at Buffalo, Buffalo, NY.

Jeon, J.S., DesRoches, R., Brilakis, I. & Lowes, L.N. 2012. Modeling and fragility analysis of non-ductile RC buildings in low-to-moderate seismic zones. In J. Carrato and J.G. Burns (eds), *Proceedings of the Structures Congress 2012*: 2199-2210.

Kunnath, S.K., Hoffman, G., Reinhorn, A.M. & Mander, J.B. 1995. Gravity-load-designed reinforced concrete buildings – Part I: Seismic evaluation of existing construction. *ACI Structural Journal* 92(3): 343-354.

Mander J.B., Priestley, M.N.J. & Park, R. 1988. Theoretical stress-strain model for confined concrete. *ASCE Journal of Structural Engineering* 114(8): 1804-1826.

McKay, M.D., Conover, W.J. & Beckman, R.J. 1979. A comparison of three methods for selecting values of input variables in the analysis of output from a computer code, *Technometrics* 21(2): 239–245.

McKenna, F., Scott, M.H. & Fenves, G.L. 2010. Nonlinear finite element analysis software architecture using object composition, *ASCE Journal of Computing in Civil Engineering* 24(1): 95–107.

Melek, M. & Wallace, J.W. 2004. Cyclic behavior of columns with short lap splices. *ACI Structural Journal* 101(6): 802-811.

Mitra, N. & Lowes, L.N. 2007. Evaluation, calibration, and verification of a reinforced concrete beam-column joint model. *ASCE Journal of Structural Engineering* 133(1): 105-120.

Newmark, N.M. & Hall, W.J. 1982. *Earthquake Spectra and Design*. Berkeley, CA: Earthquake Engineering Research Institute.

Nielson, B.G & DesRoches, R.. 2007. Analytical seismic fragility curves for typical bridges in the central and southeastern United States. *Earthquake Spectra* 23: 615-633.

Padgett, J.E., Nielson, B.G. & DesRoches, R. 2008. Selection of optimal intensity measures in probabilistic seismic demand models of highway bridge portfolios. *Earthquake Engineering and Structural Dynamics* 37: 711-725.

Pantelides, C.P., Hansen, J., Nadauld, J. & Reaveley, L.D. 2002. Assessment of reinforced concrete building exterior joints with substandard details. *PEER Report 2002/18* Pacific Earthquake Engineering Center, University of California, Berkeley, CA.

Ramamoorthy, S.K., Gardoni, P. & Bracci, J.M. 2006. Probabilistic demand models and fragility curves for reinforced concrete frames. *ASCE Journal of Structural Engineering* 132(10): 1563-1572.

Reese, R.C. 1965. *CRSI Design Handbook Volume II – 1963 ACI Code, Working Stress Method*. Chicago, IL: Concrete Reinforcing Steel Institute.

Rix, G.J. & Fernandez, J.A. 2006. *Probabilistic Ground Motions for Selected Cities in the Upper Mississippi Embayment.* http://geosystems.ce.gatech.edu/soil_dynamics/research/groundmotionsembay/

Taftali, B. 2007. *Probabilistic seismic demand assessment of steel frames with shape memory allow connections*. Ph.D. thesis, School of Civil and Environmental Engineering, Georgia Institute of Technology, Atlanta, GA.

Walker, S.G. 2001. *Seismic performance of existing reinforced concrete beam-column joints*. M.Sc. thesis, Department of Department of Civil and Environmental Engineering, University of Washington, Seattle, WA.